Jilin Daxue Xuebao (Gongxueban)/Journal of Jilin University (Engineering and Technology Edition)
ISSN: 1671-5497
E-Publication: Online Open Access
Vol: 42 Issue: 07-2023
DOI 10.17605/OSF.IO/9EF5H

STUDY OF URBAN HEAT ISLAND EFFECT IN LAHORE, PAKISTAN BY USING THERMAL VARIANCE (2000-2020)

AISHA KHAN
Department of Environmental Sciences, Fatima Jinnah Women University, Pakistan.
Corresponding Author E-mail: aishahayat85@yahoo.com

SHEIKH SAEED AHMAD
GIS and Remote Sensing Research Lab, Department of Environmental Sciences, Fatima Jinnah women University, Pakistan. E-mail: drsaeed@fjwu.edu.pk

Abstract

Natural and human induced changes to the earth surface are the main cause of thermal heterogeneity of earth's surface. Remotely sensed thermal infrared (TIR) data for determining Land Surface Temperature (LST) allows continuous global coverage that enables the assessment and quantification of these variations. The current study was designed with the goal of determining UHI in the metropolitan Lahore. i.e., the provincial capital of Punjab, Pakistan. Developing a broad-ranged, multidimensional, economically viable long-term policy to address difficulties originating from changes in the microclimate of urban areas necessitates a thorough understanding of spatiotemporal variations in LST of the region of concern. Therefore, from 2000-2020, the LST of Lahore was determined using Landsat 5 and Landsat 8 OLI images. NDVI, NDBI, Built-up Index (BUI) and NDWI results indicated the definite increase in spatial coverage of LST in Lahore and LULC identified the increasing trend in built-up area. The role of climatological variables and increasing urban population and population density on the LST and UHI of Lahore were also investigated. This facilitated the understanding of complicated interactions of LST with various physical, climatological and social factors of the city.

Index Terms: Built Environment, Land Surface Temperature, Land Use Land Cover Changes, Meteorological changes, Micro-climate, Remote Sensing, Urban Heat Island Effect

1. INTRODUCTION

The fast rising urbanisation process is one of the leading sources of increase in the number of new buildings and subsequently prompting the natural land surfaces to be replaced with impermeable surfaces like concrete, cement, asphalt etc. [1]. As a result, the energy, water, and material exchange mechanisms governing between the ground surface and the atmosphere also shift. This results in the exhaustion of large amount of heat in the urban boundary layer instigating the establishment of a distinct micro-climatic effect that causes a higher temperature in the urban area as compared to its surrounding areas. This resulting phenomenon is known as the "urban heat island (UHI) effect" [2].

Meteorological conditions, land cover types (LCTs), urban area size, and human heat sources all play a role in the establishment of urban heat islands [3], [4], [5], [6], [7]. It is critical to identify and quantify the factors that cause UHI in a particular location in order to build scientific urban plans that emphasize the appropriate distribution of industries among cities and a strategically constructed roadways and other transport networks to assist dissipate the effects of heat. As a result, the research of UHI effects spans all stages of urban growth, including single cities, megacities, and city agglomerations.

Jilin Daxue Xuebao (Gongxueban)/Journal of Jilin University (Engineering and Technology Edition)
ISSN: 1671-5497
E-Publication: Online Open Access
Vol: 42 Issue: 07-2023
DOI 10.17605/OSF.IO/9EF5H

Because of the ramifications of UHI for population and climate, and vice versa, global interest in UHI has skyrocketed in recent decades. Multiple heat island-based studies have been conducted in megacities such as London, Tokyo, and New York, which vary in physical, geographical, and sociological aspects. This phenomenon's scope is more than its seemingly straightforward scientific definitions and explanations [8]. Due to the constantly changing environment and the effects of global warming, accurate and competently established UHI is the foundation of successful, progressive, and sustainable urban developmental planning. According to Oke (1982) during the formation of a city, changes in mass, momentum, moisture and surface-air heat exchanges takes place that leads to disturbances in regional and local weather. This results in a particular urban climate in that particular area [9].

In terms of local and regional climate, the presence of a city is equivalent to the presence of a complex, spatially heterogeneous mosaic with distinctively diverse land cover and land-use classes. These classes have varying thermal values in comparison to its surroundings semi-urban and rural areas [10]. Numerous factors contribute to the construction of a city's macroclimate and built-environment, resulting in several forms of UHIs. As a result, the analysis of these many forms of urban heat islands differs in terms of the practices, instruments, and technologies used, depending on the specific aims linked to that specific place. However, the dynamics of urban micro-climate are better understood by determining the LST and LULC and their impacts on the prevailing UHI of the metropolitan area by utilising thermal infrared (TIR) radiations (8-15 micrometre) satellite imaging. The determination of the distribution of land use land cover changes of a particular area, the variations in land surface temperature using spatial analyses techniques provides the contributing effect of impenetrable and compactly built-up urban surfaces in the development of urban heat island effect in that particular area [11]. This information, along with the information from climate and environmental variables such as urban morphology, vegetation coverage, meteorological variables and social variables help in defining homogeneous zones. All of this data is then efficiently utilized in the formation of a beneficial framework for sustainable and progressive urban development planning by determining strategies to reduce UHI effect, particularly when considering climate change adaptation [12], [13].

2. METHODOLOGY

2.1 Study Area

Lahore, Pakistan's second largest city in terms of population, is the capital and largest district of the Punjab province [14]. It is the 22nd largest city in the world [15]. Lahore metropolitan is the province's most developed district, and the 2017 census revealed that its population is totally urban. Lahore is also Pakistan's only megacity, with a population that has more than doubled between 1998 and 2017, rising from 5.14 million to 11.13 million [16], [17].

Jilin Daxue Xuebao (Gongxueban)/Journal of Jilin University (Engineering and Technology Edition)
ISSN: 1671-5497
E-Publication: Online Open Access
Vol: 42 Issue: 07-2023
DOI 10.17605/OSF.IO/9EF5H

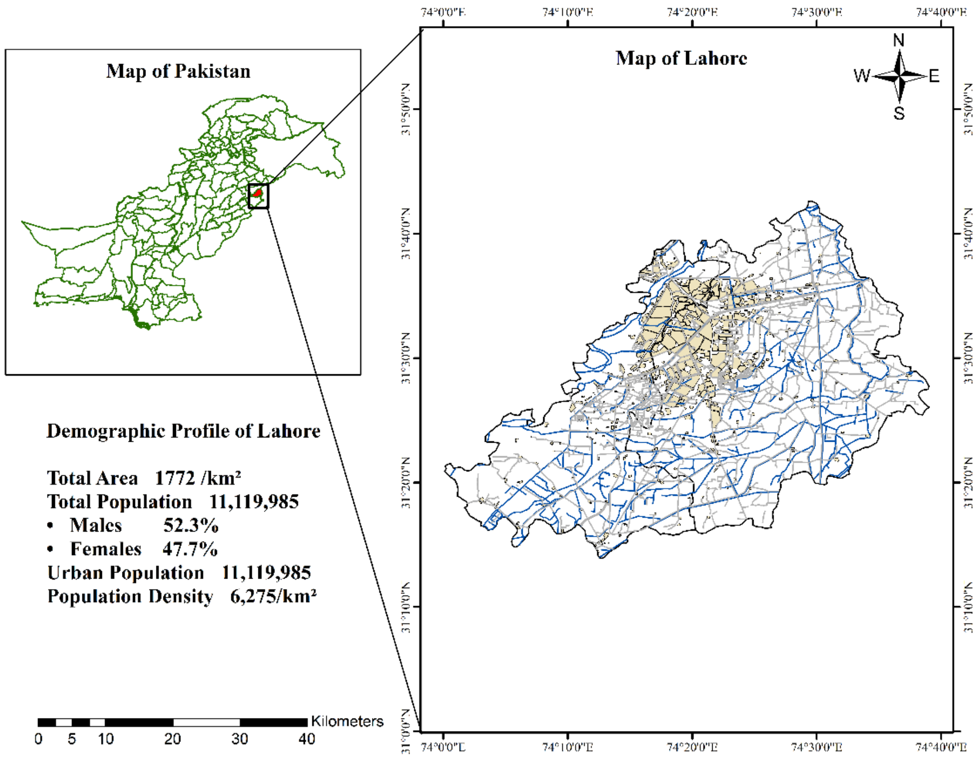

Fig 1: Demographic Profile and Map of Study Area Lahore

2.2 Methodology

Because of its complicated relationship with numerous features and characteristics of the Earth at the surface and atmospheric levels, LST is used in many environmental applications and research studies such as climate studies, agriculture studies, hydrology, and so on. Fig 2 depicts the assessment approach and aims to specify the methods chosen for each component of the overall process based on remotely sensed data to determine the temperature of the surface of the using imagery from the Landsat series of satellites (5 & 8) and statistical techniques to obtain the required parameters and indices for the study.

Jilin Daxue Xuebao (Gongxueban)/Journal of Jilin University (Engineering and Technology Edition)
ISSN: 1671-5497
E-Publication: Online Open Access
Vol: 42 Issue: 07-2023
DOI 10.17605/OSF.IO/9EF5H

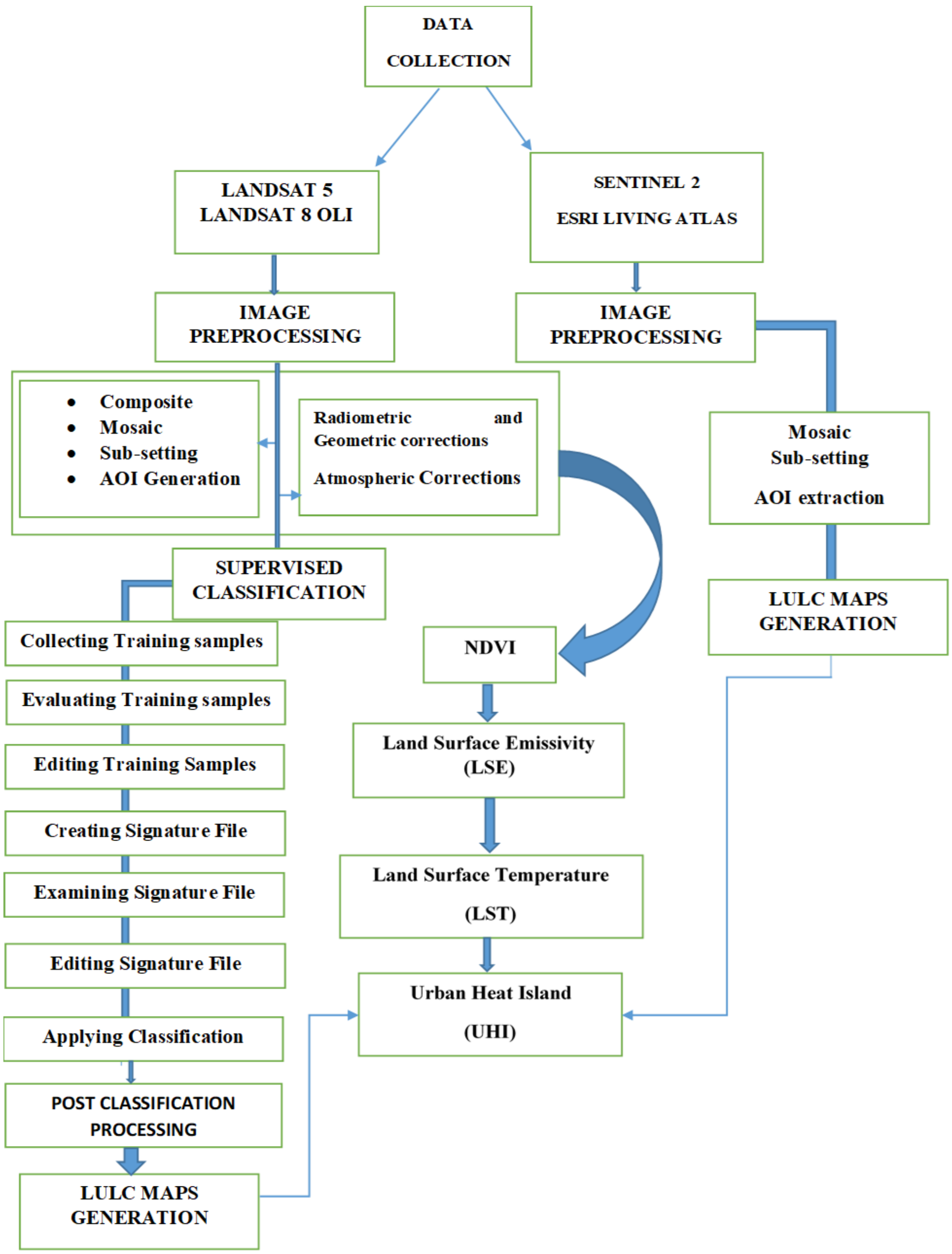

Fig 2: Flowchart of Methodology

2.3 Data Collection

The remotely sensed photos are collected from the USGS Earth Explorer webpage in order to establish the LST of the research location. Remotely sensed images obtained for district Lahore for the years 2000, 2008 and 2010 were Landsat-5 Thematic Mapper (TM) images and for years 2013, 2015-2020 the images were obtained from Landsat 8 OLI (Table 1).

Jilin Daxue Xuebao (Gongxueban)/Journal of Jilin University (Engineering and Technology Edition)
ISSN: 1671-5497
E-Publication: Online Open Access
Vol: 42 Issue: 07-2023
DOI 10.17605/OSF.IO/9EF5H

Table 1: Landsat Image Data Collected for District Lahore 2000-2020

Study Area Row/Path		Lahore 149/036
Year	**Date**	**Sensor**
2000	May 30	TM
2008	June 05	TM
2010	May 26	TM
2013	May 18	OLI
2015	May 24	OLI
2016	May 26	OLI
2017	May 29	OLI
2018	June 01	OLI
2019	May 19	OLI
2020	May 21	OLI

2.3 Extraction and Data Processing

The paper map of District Lahore was scanned, digitized and georeferenced in ArcMap 10.8 to obtain shape file to obtain study area map. In ArcGIS, the Landsat images were preprocessed. Radiometric and geometric corrections were performed. Image composite were prepared for each image and subsetting was done to extract AOI. The sub datasets were prepared from the NASA Power data sets to perform the analysis according to the requirement of this study. The Urban heat island effect in the study area was ascertained thoroughly by determining various factors and indices for the duration of 2000-2020 for study area. This include LST, NLST, NDVI, NDBI, BUI, NDWI and NDBLI.

2.4 Calculations

The steps involved in the calculations and formulae used are briefly described as follows.

2.4.1 Conversion of DN to radiance

After the preprocessing of the images the analysis of the images was done in ArcGIS 10.8. The first step in obtaining the LST from the images is the conversion of Digital Number (DN) to Top of the Atmosphere (ToA) spectral radiance. Landsat TM and ETM+ sensors convert the captured reflected solar energy into radiance and rescale it into an 8-bit Digital Number (DN) without any units and a value ranged between 0-255. The equation used for this conversion is as follows [18]:

$$\boldsymbol{L_\lambda = \frac{LMAX_\lambda - LMIN_\lambda}{QCALMAX - QCALMIN} X\,(DN - QCALMIN) + LMIN_\lambda} \qquad \textbf{(1)}$$

Where,

L_λ = Spectral Radiance W/m^2

$LMAX_\lambda$ = Spectral radiance for each band at digital number 255

$LMIN_\lambda$ = Spectral radiance for each band at digital number 0

QCALMAX = 255

Jilin Daxue Xuebao (Gongxueban)/Journal of Jilin University (Engineering and Technology Edition)
ISSN: 1671-5497
E-Publication: Online Open Access
Vol: 42 Issue: 07-2023
DOI 10.17605/OSF.IO/9EF5H

QCALMIN = 0

DN = Quantized calibrated pixel value

It can also be determined as follows:

$$L_\lambda = M_L Q_{CAL} + A_L \quad (2)$$

Where,

L_λ = Spectral Radiance W/m^2

M_L = Gain (0.067 for Landsat 7 & 0.00033420 for Landsat 8)

Q_{CAL} = Quantized calibrated pixel value [DN]

A_L = Offset (-0.06709 for Landsat 7 and 0.1 for Landsat 8)

2.4.2 Conversion of Spectral Radiance to Brightness Temperature

The radiance of the electromagnetic radiation travelling upward from the top of the atmosphere is defined as the Brightness temperature [19]. The second step is the conversion of the spectral radiance obtained (Eq 1 & 2) to Brightness temperature [20]. The equation for this purpose is as follows:

$$T = \frac{K_2}{ln(K_1/L_\lambda + 1)} \quad (3)$$

Where,

T = Brightness temperature of the satellite (K)

L_λ = Spectral Radiance W/m2

K_1 and K_2 = Thermal band conversion constants

Band 6: 606.76 and 1260.56 & Band 10:774.89 and 1321.08

The temperature obtained is in Kelvin. This temperature is then converted from Kelvin to Celsius as follows

$$T_2 = T_1 – 273.15 \quad (4)$$

Where,

T_2 = Brightness temperature in ^0C

T_1 = Brightness Temperature in Kelvin

2.4.3 Retrieval of Land Surface Temperature

Land Surface Temperature (LST) was determined by using the equation that is based on Brightness Temperature (T_b) and the emissivity (Ɛ). The equation used for the derivation of Land Surface Temperature from the Landsat images is presented as follows [21]:

$$S_t = \frac{T_B}{1 + (\lambda \, x \, \frac{T_B}{\rho}) In\varepsilon} \quad (5)$$

Jilin Daxue Xuebao (Gongxueban)/Journal of Jilin University (Engineering and Technology Edition)
ISSN: 1671-5497
E-Publication: Online Open Access
Vol: 42 Issue: 07-2023
DOI 10.17605/OSF.IO/9EF5H

Where,

S_t = Land surface temperature (LST)

T_b = Brightness temperature

λ = Wavelength of emitted radiance

ρ = h x $\frac{c}{\sigma}$ = (1.438 x 10^{-2} m K)

σ = Boltzmann's constant (1.38 x 10^{-23} J/K)

h = Planck's constant (6.626 x 10^{-34})

c = velocity of light (20998 x 10^{8} m/s)

Ɛ = Land Surface Emissivity

As indicated by the equation 5, in order to obtain the LST, the emissivity must also be calculated. This can be done as followed:

Retrieving Normalized Difference Vegetation Index (NDVI)

Normalized difference vegetation index (NDVI) is a unitless, dimensionless graphical indicator. It is a ratio between Red (R) and Near Infra-Red (NIR) bands of radiation and is mostly utilized for the remotely sensed analysis to determine health of vegetation is useful in understanding vegetation density [22]. The vegetation absorbs more red radiation and strongly reflect NIR radiation. The values of NDVI range from +1 (dense leafy green vegetation) to −1 (generally water bodies). NDVI is calculated as follows [19]:

$$\boldsymbol{NDVI} = \frac{NIR-RED}{NIR+RED} \qquad \textbf{(6)}$$

Determining Vegetation Proportion

The vegetation Proportion (P_v) also known as Fractional vegetation cover (FVC) is an important vegetation biophysical variable. It is the ratio of vertically projected area of vegetation on the ground to the total surface extent of vegetation area. Together with NDVI, the P_v obtained is used to estimate the emissivity [23]. The vegetation proportion is determined as follows:

$$\boldsymbol{P_v} = \left(\frac{NDVI- NDVI_{min}}{NDVI_{max}- NDVI_{min}}\right)^2 \qquad \textbf{(7)}$$

Where,

P_v = Vegetation proportion

NDVI = Normalized Difference Vegetation Index

Retrieving Land Surface Emissivity (LSE)

A major parameter to obtain Land surface temperature is Land surface emissivity (LSE). As a mixture of bare soil and vegetation comprises a pixel from which the NDVI index range was obtained [24].

Jilin Daxue Xuebao (Gongxueban)/Journal of Jilin University (Engineering and Technology Edition)
ISSN: 1671-5497
E-Publication: Online Open Access
Vol: 42 Issue: 07-2023
DOI 10.17605/OSF.IO/9EF5H

The Ɛ for the pixel is calculated as follows:

$$\varepsilon = 0.004\ P_v + 0.986 \quad (8)$$

Where,

Ɛ	=	Land Surface Emissivity		
P_v	=	Vegetation proportion		
0.004	=	ε_s	=	Emissivity of soil
0.986	=	ε_v	=	Emissivity of vegetation

2.4.4 Calculation of Indices for UHI

Normalized Land Surface Temperature (NLST)

The normalized Land Surface Temperature is used to provide visual interpretation of predetermined LST on the basis of objective information. It determines the spatial distribution of the extracted land surface temperature values from the images obtained from the satellites [25]. It is determined as follows:

$$\boldsymbol{NLST} = \left(\frac{LST_i - LST_{min}}{LST_{max} - LST_{min}}\right) \quad (9)$$

Where,

LST_i = Pixel value of LST in the observed scene

LST_{min} = Lowest value of LST in the observed scene

LST_{max} = Highest value of LST in the observed scene

Normalized Difference Built-up Index (NDBI)

NDBI is determined using the Near infrared radiation band (NIR) and Shortwave Infrared radiation band (SWIR) This ratio is determined to alleviate the terrain illumination variations and atmospheric impacts. The equation used to determine the NDBI is as follows [26]:

$$\boldsymbol{NDBI} = \frac{SWIR - NIR}{SWIR + NIR} \quad (10)$$

Built-Up Index (BUI) Retrieval

The BUI was calculated by determining the difference between the NDVI and NDBI map layers as followed [27]:

$$\mathbf{BUI = NDBI - NDVI} \quad (11)$$

Normalized Difference Water Index (NDWI)

NDWI is a satellite-derived index from the Near-Infrared (NIR) and Short-Wave Infrared (SWIR) channels. The strong absorbability and low radiation of water bodies in visible to NIR range and its sensitivity to built-up area made it the most appropriate index for the mapping of water bodies in the study area. NDWI is determined as follows [28]:

Jilin Daxue Xuebao (Gongxueban)/Journal of Jilin University (Engineering and Technology Edition)
ISSN: 1671-5497
E-Publication: Online Open Access
Vol: 42 Issue: 07-2023
DOI 10.17605/OSF.IO/9EF5H

$$NDWI = \frac{GREEN - NIR}{GREEN + NIR} \quad (12)$$

Normalized Difference Bare Land Index (NDBLI)

The rapidly changing land cover, particularly the spatiotemporal changes in bare land, is an indicator of anthropogenic activities in a developing city. NDBLI is an important index for determination of such changes as the red band has a high contrast between the bare land and other classes due to its much higher DN values. The equation to determine the Normalized difference Bare Land Index is as follows [29], [30]:

$$NDBLI = \frac{RED - TIR}{RED + TIR} \quad (13)$$

3. RESULTS AND DISCUSSION

3.1 Land Surface Temperature of Lahore (2000-2020)

The minimum LST of Lahore in 2000 was 15.65 ^{o}C and maximum LST was 35.67 ^{o}C. The majority of the area of Lahore occur in the LST range of 28.76 ^{o}C - 35.67 ^{o}C (Fig. 3.). The difference between the urban and rural LST is 2.31 ^{o}C indicating the UHI in the area.

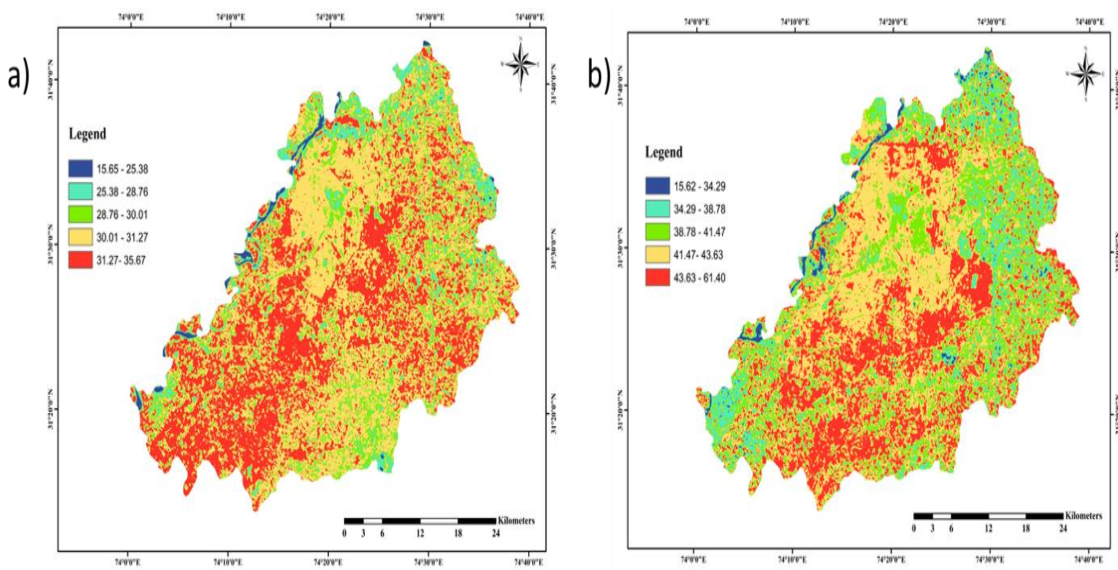

Fig 3: Land Surface Temperature of Lahore a) 2000 and b) 2020

In 2008, the minimum LST has increased by 6.73 ^{o}C from its value in 2000. The increase in maximum LST is by 1.17 ^{o}C. In 2010, the LST of Lahore increased by 24.36 ^{o}C of its value in 2000 and by 23.19 ^{o}C from its value in 2008. The minimum and maximum Land Surface Temperature (LST) exhibited by Lahore from 2000 to 2020 is given in fig. 4.

Jilin Daxue Xuebao (Gongxueban)/Journal of Jilin University (Engineering and Technology Edition)
ISSN: 1671-5497
E-Publication: Online Open Access
Vol: 42 Issue: 07-2023
DOI 10.17605/OSF.IO/9EF5H

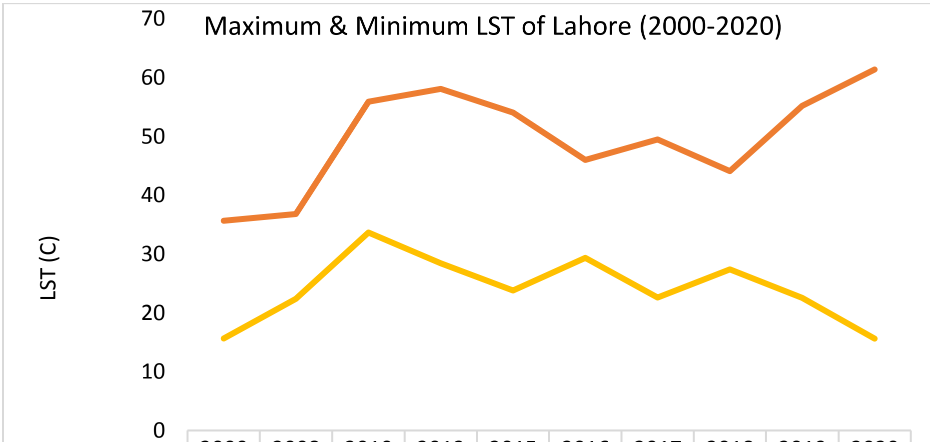

	2000	2008	2010	2013	2015	2016	2017	2018	2019	2020
LST Max	35.67	36.84	55.94	58.09	54.05	46.03	49.51	44.11	55.23	61.4
LST Min	15.65	22.39	33.67	28.44	23.81	29.38	22.6	27.42	22.58	15.62

Fig 4: Maximum and Minimum Land Surface Temperature of Lahore (2000-2020)

2010 was the year of a destructive flood in most parts of Pakistan. Upper atmosphere changes leading to the formation of Meso-scale convective system (MCS), resulted in heavy rains and consequential flood s in the most parts of Khyber Pakhtunkhwa, Balochistan, Lower Punjab and Sindh [31], [32], [33]. In the duration of 1996-2015, Pakistan was number seven in Climate Risk Index (CRI) [34]. Therefore, global climatic changes were a major reason behind the destructive and unprecedented floods in 2010 and 2011 in Pakistan [35].

The impacts of the changes in weather have also been observed in Lahore as in April 2010, the city observed the highest temperature for April in Lahore i.e., 44 ^oC [36]. The air temperature is usually higher in the regions around the flooding regions as well [37]. Imran & Aqsa (2020) research on urban climate of Lahore also showed the increasing trend being observed in the LST of Lahore (1996-2016) [38].

In 2013 (Fig. 4.), the minimum LST of Lahore increased to 28.44 ^oC from 24.12 ^oC observed in 2010 and 15.65 ^oC observed in 2000. The maximum LST became 58.09 ^oC, which was less than the value observed in 2010 but 22.42 ^oC higher than the LST observed in 2000. A further decreased in the LST was observed in 2015 (Fig.4.). The minimum LST scaled down to 23.81 ^oC and the minimum LST range also came down to 23.81 ^oC -31.28 ^oC. This range is less than the range of minimum LST that was observed in 2013 (28.44 ^oC -40.07 ^oC). In the year 2015, the global land surface temperature average was 1.33 ^oC above the 20th century average LST that broke the global LST records for 2007 and 2010 as well [39].

Most of the area of Lahore exhibited the LST range of 36.14 ^oC -54.05 ^oC. The LST around the water bodies decreased from 28.44 ^oC -40.07 ^oC range to 23.81 ^oC -31.28 ^oC. Kafy et al., (2021), investigated the urban thermal environment changes of Chattogram city, Bangladesh and found that along with the increase in UHI and LST of urban built-up area, the mean LST of water bodies also exhibited an increasing trend between 1999-2019 [40]. The research done by Feng et al., (2018) on Taihu lake basin of China, also showed

Jilin Daxue Xuebao (Gongxueban)/Journal of Jilin University (Engineering and Technology Edition)
ISSN: 1671-5497
E-Publication: Online Open Access
Vol: 42 Issue: 07-2023
DOI 10.17605/OSF.IO/9EF5H

that water body LST has increased, even if the rate of increase is lowest while considering the rise in other classes like built area, bare land and even vegetation [41].

2017 was another year for global weather anomalies that lead to various extreme weather events like flash floods, droughts, wild fires, high temperatures etc. the LST of Lahore, however, continued exhibiting a decreasing trend. The value was still above the year 2000 value but less than the range that was observed in 2015. The minimum LST in 2017 was 22.59 ^{o}C. In contrast, in 2018, the minimum LST observed an abrupt increase in its value from 22.59 ^{o}C to 27.41 ^{o}C.

The maximum LST, however, decreased from 49.50 ^{o}C to 44.11 ^{o}C. These types of abrupt changes are not an uncommon event as LST depends on multiple local, regional and global factors. Any change in one of these factors can lead to the variation in LST of an urban area [42], [43]. The minimum LST again decreases in 2019 to 22.58 ^{o}C (Fig. 4.). The minimum LST range decreased from 27.41-33.24 to 22.58 ^{o}C -29.87 ^{o}C.

In 2020, the minimum LST became even less than its value in 2000 by 0.03 ^{o}C. The minimum LST range, however exhibited an increase by 8.91 ^{o}C. This indicated the presence of UHI in the area (Fig. 3.). The maximum LST increased by 25.73 ^{o}C. In 2000, the major area of Lahore exhibited an LST range of 30.01 ^{o}C to 35.67 ^{o}C. In 2020, the majority of Lahore existed in the LST range of 38.78 ^{o}C -61.40 ^{o}C. This not only indicated the LST by increasing value but the spatial coverage of high temperature LST had also increased.

The LST increase is by 1.23 ^{o}C/year approximately. Also, unlike cities like Melbourne, Tokyo, New York, Dublin, Oslo [44], Tehran [45], United Arab Emirates [46] and three hundred cities of China [47] where the investigation on the impacts of COVID-19 related lockdown on environment and found that the lockdown had resulted in decrease in UHI and Greenhouse gases decreasing both the SUHI and canopy layer heat island effect in the cities, the impact of COVID-19 lockdown decrease in anthropogenic activities were only visible in the minimum LST as it reverted to its original value of 2000 [19].

3.2 Visual Representation of Indices (2000-2020)

The visual interpretation of the various indices including the NDVI, NDBI, BUI, NDWI (Fig. 5.), NLST and NDBLI (Fig. 6.) for 2000 and 2020 for Lahore are provided below. These figures clearly highlight the changes in the built area in Lahore in the given time range.

Jilin Daxue Xuebao (Gongxueban)/Journal of Jilin University (Engineering and Technology Edition)
ISSN: 1671-5497
E-Publication: Online Open Access
Vol: 42 Issue: 07-2023
DOI 10.17605/OSF.IO/9EF5H

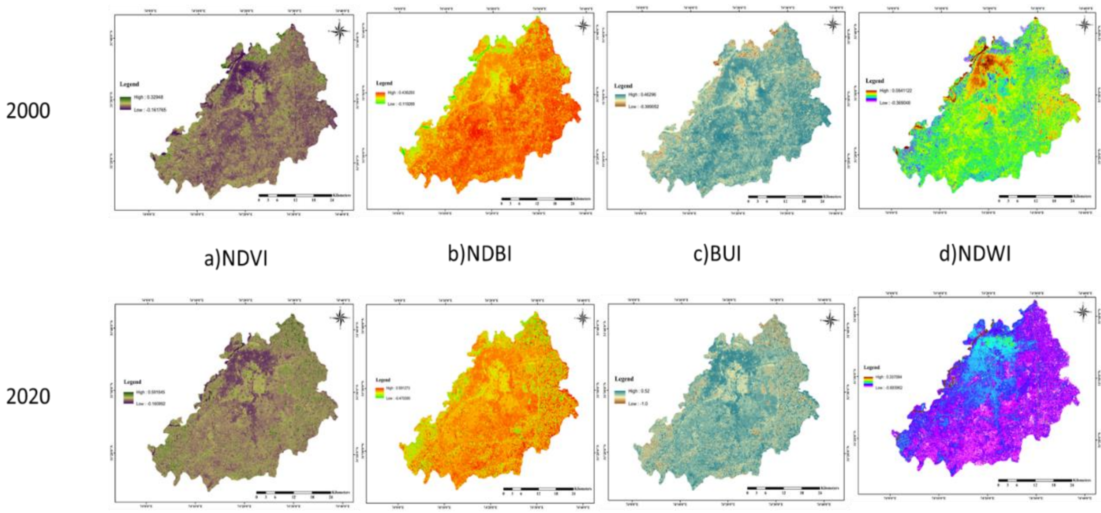

Fig 5: Visual Representation of Indices of Lahore (2000-2020) a) Normalized Difference Vegetation Index b) Normalized Difference Built-up Index c) Built-Up Index d) Normalized Difference Water Index

Fig 6. Provides the Normalized Land Surface Temperature of Lahore and the Normalized Difference Bare-Land Index of Lahore from 2000-2020

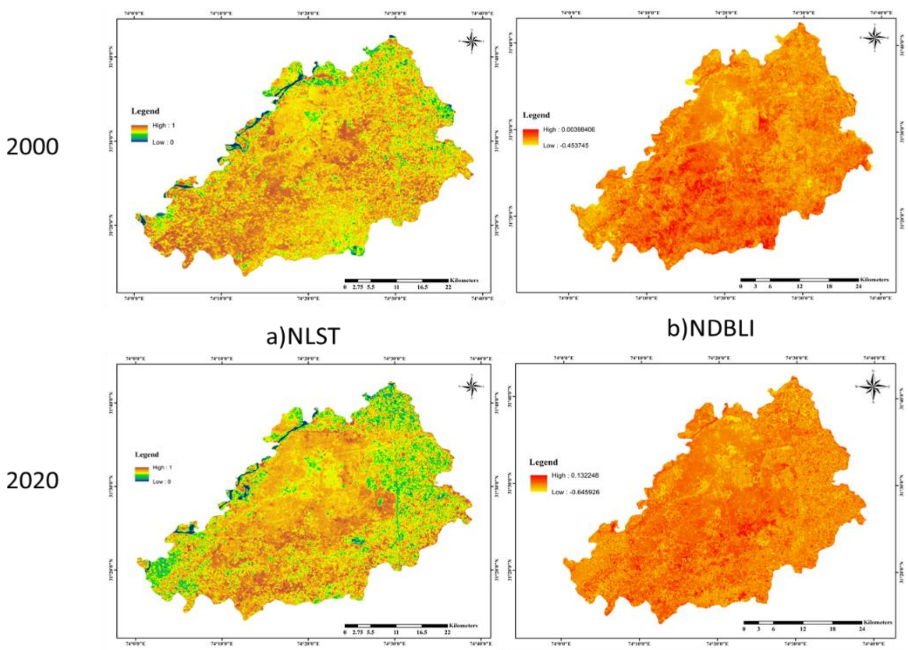

Fig 6: a) NLST (2000-2020) of Lahore and b) NDBLI (2000-2020) of Lahore

3.3 Land Use/Land Cover Change (LULC) of Lahore 2000-2020

Fig. 7. (a) And (b) provides the visual interpretation of LULC of Lahore in 2000 and 2020 respectively. The biggest shift in Lahore's LULC is the growth in built-up area and decrease in vegetation area. Mumtaz et al., (2020) studied the spatiotemporal LULC variations in Lahore (1998-2018) and discovered that the built-up area increased while

Jilin Daxue Xuebao (Gongxueban)/Journal of Jilin University (Engineering and Technology Edition)
ISSN: 1671-5497
E-Publication: Online Open Access
Vol: 42 Issue: 07-2023
DOI 10.17605/OSF.IO/9EF5H

vegetation declined [48]. The built-up area is likely to grow further due to the ongoing residential and commercial expansion in Lahore. The addition of these regions raises Lahore's built-up area percentage, as exhibited by the LULC year average shown in Fig.7. (c). increasing the built-area to 752.8 sq.km approximately [49].

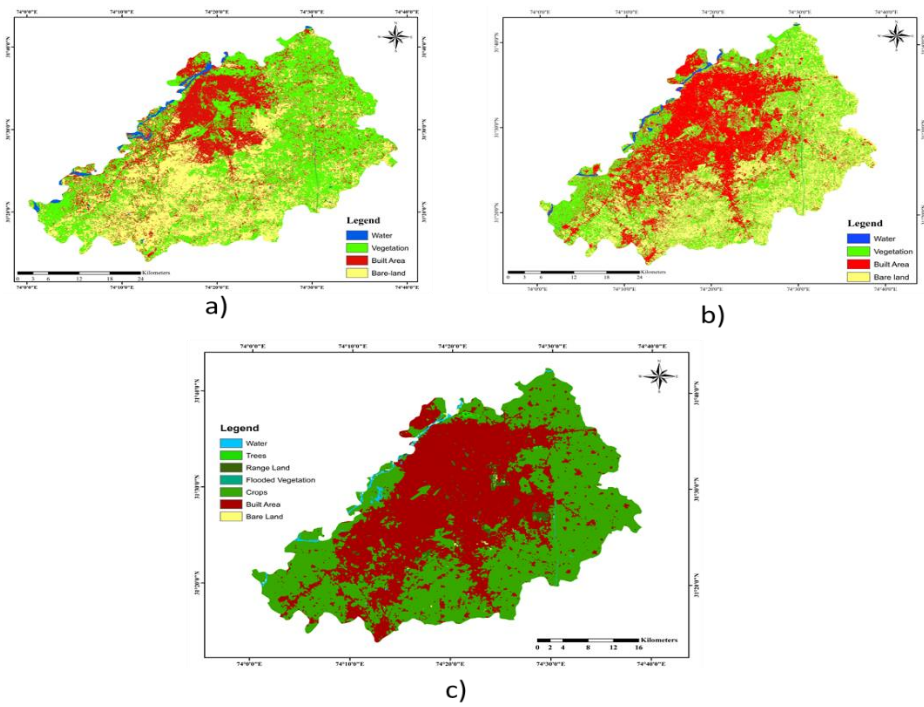

Fig 7: a) LULC of Lahore in 2000 b) LULC of Lahore in 2020 c) Average LULC of Lahore in 2020 from Esri Living Atlas

The percentage changes observed in feature classes of Lahore are provided in the Fig. 8.

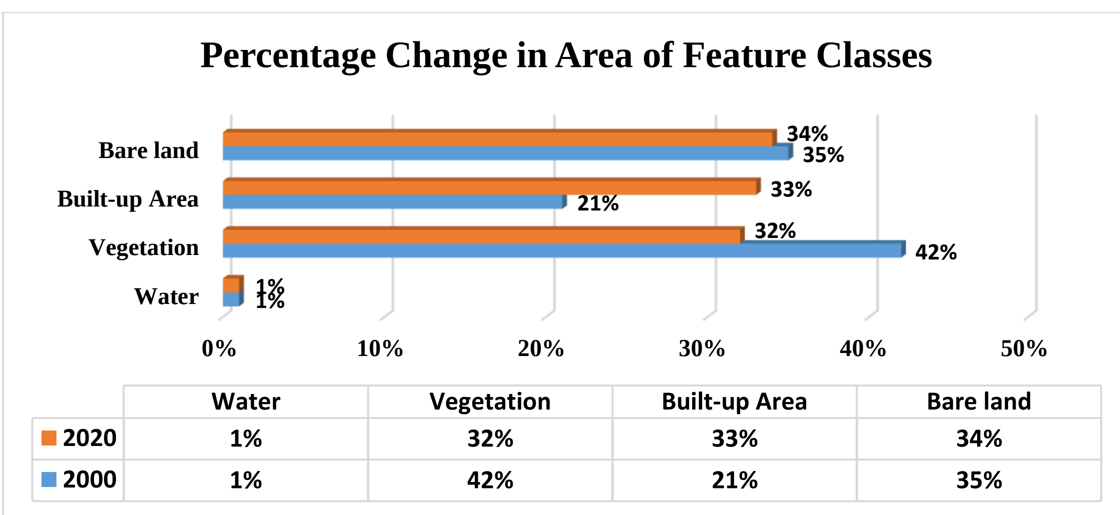

	Water	Vegetation	Built-up Area	Bare land
2020	1%	32%	33%	34%
2000	1%	42%	21%	35%

Fig 8: Percentage Change in the Area of Feature Classes of Lahore (2000-2020)

ISSN: 1671-5497
E-Publication: Online Open Access
Vol: 42 Issue: 07-2023
DOI 10.17605/OSF.IO/9EF5H

3.4 Meteorological Results

The earth skin temperature and maximum and minimum temperature of Lahore, didn't show any abrupt changes. The values of earth skin temperature and maximum and minimum temperatures follow a similar pattern (Fig. 9. (a)). The temperature changes for each month follows a narrow range with temperature of June as the highest and January as the lowest temperature months. The variations are also within a narrow range, except for the February and April. The overall temperature remains below 45 ^{o}C (Fig. 9. (b)).

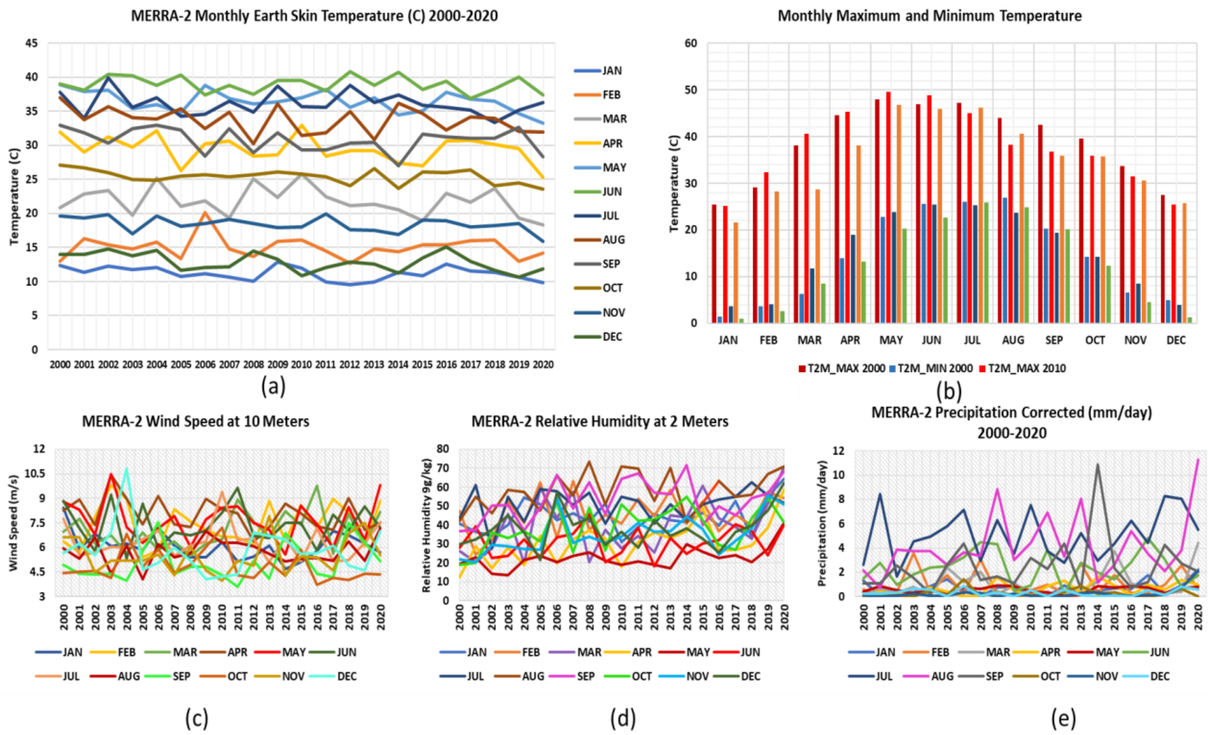

Fig 9: Meteorological Variables of Lahore (2000-2020) a) MERRA-2 Monthly Earth Skin data b) maximum and Minimum Monthly Temperature of 2000, 2010 and 2020 c) MERRA-2 Wind Speed at 10 meters d) MERRA-2 Relative Humidity at 2 meters e) MERRA-2 Corrected Precipitation of Lahore

The windspeed in Lahore is more than 3 m/s for all the months (Fig. 9. (c)). The wind speed is ideal for driving the warm air away from the urban area but the urban core of Lahore is densely built and extended to its boundaries, therefore, the UHI still exist in Lahore. While determining the impacts of multiple factors on the UHI of Seoul, Korea, Ngarambe et al., (2021) stated that despite the fulfilling of one UHI decreasing criteria, the UHI still impact the urban area as there are numerous other factors that will be responsible for the increase of UHI for example the wind speed alone will not be enough, the terrain, urban morphology, the congested built-up etc. would still hinder the proper ventilation from the urban area, hence, increasing the UHI of the urban area [50].

The precipitation levels in Lahore were maximum values in the months of July and August, followed by June, September and February. The remaining months are below 2 mm/day.

Jilin Daxue Xuebao (Gongxueban)/Journal of Jilin University (Engineering and Technology Edition)
ISSN: 1671-5497
E-Publication: Online Open Access
Vol: 42 Issue: 07-2023
DOI 10.17605/OSF.IO/9EF5H

The minimum precipitation is for October 2020 which was recorded as zero mm/day. The maximum precipitation was also for 2020 and it was in the month August having the volume of 11.26mm/day. The second peak is observed for September 2014 at the volume of 10.88 mm/day. The third and fourth highest peaks were for August 2008 at 8.84 mm/day and July 2001 at 8.47 mm/day (Fig. 9. (e)).

The humidity in Lahore have increased from its value in 2000 (Fig. 9. (d)). The humidity was higher in the months of July, august and September in 2010 as well. Humidity has increased for all the months in 2020. The correlation of these factors with the UHI is also dependent upon multiple factors, particularly when considering the summer UHI in densely populated and densely built urban area.

Peng et al., (2019) studied the spatiotemporal patterns of UHI in different locations of China and their findings showed that the different locations have different intensity of the UHI depending upon the prevalent actors in the area. The intensity will not only be different for urban/rural areas, it would also be different according to the physical characteristics of the urban area with respect to the meteorological factors [51].

3.5 Population

The population dwelling in an urban area is known as the urban population and can be used as a replacement indication of the physical structure of that urban region (city). This is because an increase in population can be connected to an increase in urban built area building and energy usage [52], [53]. T

he rise in population produces urban migration, which reduces vegetative cover and available bare land, however the rate of urbanisation does not always correspond with the increase in urban area by expanding beyond the municipal boundaries. This causes urban area congestion due to the increased need for tightly developed urban services infrastructure [19].

The elements driving all of these developments include increased urbanisation caused by unplanned urban population growth. The increase in the population of Lahore is from 5,576,000 (2000) to 12,642,000 (2020) with the percentage increase of 126.72% (Fig 10. (a)). The population projections for Lahore indicates the further increase in population to 19,117,000 respectively (Fig. 10. (b)).

The population of Lahore increase by 51.22 % from 2020 to 2035 and 242.84% from 2000-2035. That increase in population will result in further changes in LULC Lahore in future. Unless properly planned, these changes will lead to increase in UHI effect leading to other environmental impacts like, air pollution, heat waves and health impacts due to both thermal discomfort and air pollution.

Jilin Daxue Xuebao (Gongxueban)/Journal of Jilin University (Engineering and Technology Edition)
ISSN: 1671-5497
E-Publication: Online Open Access
Vol: 42 Issue: 07-2023
DOI 10.17605/OSF.IO/9EF5H

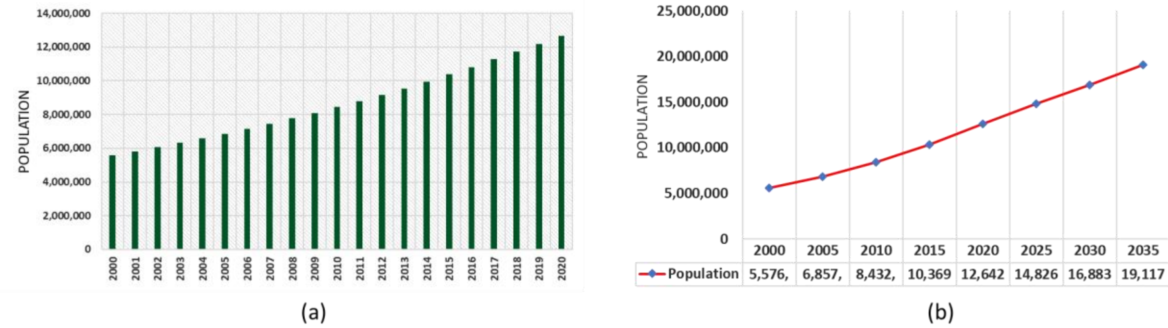

Fig 10. a) Population of Lahore (2000-2020) b) Population Projection of Lahore 2000-2035

4. CONCLUSION

The purpose of this study was to show the importance of the relationship between the urban heat island effect and microclimate fluctuations, recognise and comprehend the factors that contribute to current changes in urban microclimates, as well as identify difficulties, so that planners and policymakers are better prepared for sustainable future urban design. As unplanned growth causes problems such as the urban heat island effect, global warming, air pollution, flash floods, inadequate infrastructure facilities and services, population explosion, overuse and deterioration of available resources, and environmental degradation there is no doubt that planned urban growth is important for a country's development. As more people move to cities, urban heat mitigation will become increasingly important in order to improve human health and preserve the city's socioeconomic success. Even city-scale mitigation, adaptation, and economic measures do not rely solely on cities. Cities, nations, civic organisations, investors, and corporations are among the many actors involved in global climate adaptation and strategy. The shutdown caused by the worldwide COVID-19 epidemic presented an once-in-a-lifetime environmental chance to investigate ground conditions when human activity was minimised. Positive changes in the surroundings seen in that situation should be considered. More efforts should be made as the possibility of environmental sustainability with mitigation actions became clear.

Acknowledgment

The authors wish to thank Higher Education Commission Pakistan for the support.

Disclaimer None to Declare

Conflict of interest none to Declare

References

1) C. P. Lo, D. A. Quattrochi, and J. C. Luvall, “Application of high-resolution thermal infrared remote sensing and GIS to assess the urban heat island effect,” *International journal of Remote sensing*, vol. *18 no.* 2, pp.287-304, 1997 available at https://www.tandfonline.com/doi/abs/10.1080/014311697219079

2) T. R. Oke, “City size and the urban heat island. Atmospheric Environment,” vol. 7, no. 8, pp. 769-779, 1973, available at https://www.sciencedirect.com/science/article/abs/pii/0004698173901406

3) S. Peng, S.Piao, P. Ciais, P. Friedlingstein, C. Ottle, F. M. Bréon, H. Nan, L. Zhou and R. B. Myneni, R.B., “Surface urban heat island across 419 global big cities,” *Environmental science & technology*, vol. *46, no.* 2, pp.696-703, 2012, available at https://pubs.acs.org/doi/pdf/10.1021/es2030438

4) P. Coseo and L. Larsen, “How factors of land use/land cover, building configuration, and adjacent heat sources and sinks explain Urban Heat Islands in Chicago,” *Landscape and Urban Planning*, vol. *125*, pp.117-129, 2014, available at https://www.sciencedirect.com/science/article/abs/pii/S0169204614000607

5) N. Debbage and J. M. Shepherd, “The urban heat island effect and city contiguity,” *Computers, Environment and Urban Systems*, vol. *54*, pp.181-194, 2015, available at https://www.sciencedirect.com/science/article/abs/pii/S0198971515300089

6) G. Guo, Z. Wu, R. Xiao, Y. Chen, X. Liu and X Zhang, “Impacts of urban biophysical composition on land surface temperature in urban heat island clusters” Landscape and Urban Planning, vol. 135, pp.1-10, 2015, available at https://www.sciencedirect.com/science/article/abs/pii/S0169204614002679

7) M. Tan and X. Li, “Quantifying the effects of settlement size on urban heat islands in fairly uniform geographic areas,” *Habitat International*, vol. *49*, pp.100-106, 2015, available at https://www.sciencedirect.com/science/article/abs/pii/S0197397515000946

8) I. D. Stewart and T. R. Oke, “Local climate zones for urban temperature studies,” *Bulletin of the American Meteorological Society*, vol. *93 no.* 12, pp.1879-1900, 2012, available at https://journals.ametsoc.org/view/journals/bams/93/12/bams-d-11-00019.1.xml?tab_body=pdf

9) T. R. Oke, “The energetic basis of the urban heat island,” *Quarterly journal of the royal meteorological society*, vol. *108* no. 455, pp.1-24, 1982, available at https://www.patarnott.com/pdf/Oake1982_UHI.pdf

10) J. J. Wu, “Making the case for landscape ecology an effective approach to urban sustainability,” Landsc. J., vol. 27, pp. 41–50, 2008, available at https://lj.uwpress.org/content/27/1/41.short

11) K. Ward, S. Lauf, B. Kleinschmit and W. Endlicher, “Heat waves and urban heat islands in Europe: A review of relevant drivers,” *Science of the Total Environment*, vol. *569*, pp.527-539, 2016, available at https://www.sciencedirect.com/science/article/pii/S0048969716312931

12) B. Bechtel, M. Demuzere, G. Mills, W. Zhan, P Sismanidis, C. Small, and J. Voogt, “SUHI analysis using Local Climate Zones—A comparison of 50 cities,” *Urban Climate*, vol. *28*, p.100451, 2019, available at https://www.sciencedirect.com/science/article/abs/pii/S2212095519300239

13) L. Gutierrez, G. Garcia, M. Mendizabal and N. Peña, “Unpackaging Urban Heat Island: concepts, methods and practice examples for assessing urban climate and UHI effect to enhance planning decisions,” 2020, available at https://growgreenproject.eu/wp-content/uploads/2021/05/GrowGreen_WP3_UHI_method_Tec_140720.pdf

14) Government of Punjab, “District Profile,” 2018, available at https://lahore.punjab.gov.pk/district_profile

15) United Nations Department of Economic and Social affairs Population Dynamics (UNDES), “World’s Urbanization Prospects, 2018,” 2022.

16) Pakistan Bureau of Statistics, 2017, available at https://www.pbs.gov.pk/sites/default/files//population_census/KP%20District%20Wise.pdf

17) The Business Year (TBY), ”From Karachi to Lahore: Pakistan: 4- Top cities,” 2020, available at https://www.thebusinessyear.com/article/pakistan-top-4-four-economic-centers-cities-in-2020

18) B. Ahmed, R. Ahmed and X. Zhu, "Evaluation of model validation techniques in land cover dynamics," *ISPRS International Journal of Geo-Information*, vol. *2*, no. 3, pp.577-597, 2013, available at https://www.mdpi.com/2220-9964/2/3/577

19) N. Sahani, S. K. Goswami and A. Saha, "The impact of COVID-19 induced lockdown on the changes of air quality and land surface temperature in Kolkata city, India," Spatial Information Research, vol. 29 no. 4, pp. 519-534, 2021, available at https://link.springer.com/article/10.1007/s41324-020-00372-4

20) K. Zanter, "Landsat 8 (L8) data user's handbook, "Landsat Science Official Website, 33, 2016.

21) Q. Weng, D. Lu and J Schubring, "Estimation of land surface temperature–vegetation abundance relationship for urban heat island studies," *Remote sensing of Environment*, vol. *89* no. 4, pp.467-483, 2004, available at https://www.sciencedirect.com/science/article/abs/pii/S0034425703003390

22) A. Arabameri and H. R. Pourghasemi, "Spatial modeling of gully erosion using linear and quadratic discriminant analyses in GIS and R," In *Spatial modeling in GIS and R for earth and environmental sciences*, pp. 299-321. Elsevier, 2019, available at https://www.sciencedirect.com/science/article/abs/pii/B9780128152263000132

23) E. Neinavaz, A. K. Skidmore and R Darvishzadeh, "Effects of prediction accuracy of the proportion of vegetation cover on land surface emissivity and temperature using the NDVI threshold method," International *Journal of Applied Earth Observation and Geoinformation*, vol. *85*, p.101984, 2020, available at https://www.sciencedirect.com/science/article/pii/S030324341930618X

24) S. Ahmadi, H. Alizadeh and B. Mojaradi, "Land surface temperature assimilation into a soil moisture-temperature model for retrieving farm-scale root zone soil moisture," *Geoderma*, vol. *421*, p.115923, 2022, available at https://www.sciencedirect.com/science/article/abs/pii/S0016706122002300

25) M. F. Baqa, L. Lu, F. Chen, S. Nawaz-ul-Huda, L. Pan, A. Tariq, S. Qureshi, B. Li and Q. Li, "Characterizing Spatiotemporal Variations in the Urban Thermal Environment Related to Land Cover Changes in Karachi, Pakistan, from 2000 to 2020," Remote Sensing, vol. 14, no. 9, p. 2164 2022, available at https://doi.org/10.3390/rs14092164

26) L. Chen, M. Li, F. Huang and S. Xu, "Relationships of LST to NDBI and NDVI in Wuhan City based on Landsat ETM+ image. 6th International Congress on Image and Signal Processing (CISP), 2013," pp. 840-845, 2013, available at https://ieeexplore.ieee.org/document/6745282

27) D. Kaimaris and P. Patias, "Identification and area measurement of the built-up area with the Built-up Index (BUI)," *Int. J. Adv. Remote Sens. GIS*, vol. *5* no. 1, pp.1844-1858, 2016, available at http://ikee.lib.auth.gr/record/336133/files/Identification%20and%20Area%20Measurement%20of%20the%20Built-up%20Area%20with%20the%20Built-up%20Index%20%28BUI%29.pdf

28) S. K. McFeeters, "The use of the Normalized Difference Water Index (NDWI) in the delineation of open water features, "International journal of remote sensing, vol. 17 no. 7, pp. 1425-1432, 1996, available at https://www.tandfonline.com/doi/abs/10.1080/01431169608948714

29) H. Li, C. Wang, C. Zhong, A. Su, C. Xiong, J. Wang and J. Liu, "Mapping Urban Bare Land Automatically from Landsat Imagery with a Simple Index. Remote Sensing" vol. 9 no. 3 pp.249, 2017, available at https://doi.org/10.3390/rs9030249

30) Z. Qi, A. G. Yeh, X. Li and X. Liu, "A land clearing index for high-frequency unsupervised monitoring of land development using multi-source optical remote sensing images," ISPRS Journal of Photogrammetry and Remote Sensing, vol. 187, pp. 393-421, 2022, available at https://www.sciencedirect.com/science/article/pii/S0924271622000909?via%3Dihub

31) D. Barriopedro, E. M. Fischer, J. Luterbacher, R. M. Trigo, and R. García-Herrera, "The hot summer of 2010: redrawing the temperature record map of Europe," Science, vol. 332, no. 6026, pp. 220-224, 2011, available at https://www.science.org/doi/abs/10.1126/science.1201224

32) O. Martius, H. Sodemann, H. Joos, S. Pfahl, A. Winschall, M. Croci-Maspoli, M. Graf, E. Madonna, B. Mueller, S. Schemm, J. Sedláček, M. Sprenger, H. Wernli, “The role of upper-level dynamics and surface processes for the Pakistan flood of July 2010,” Quarterly Journal of the Royal Meteorological Society, vol. 139 no. 676, pp. 1780-1797, 2013, available at https://doi.org/10.1002/qj.2082

33) T. J. Galarneau, T. M. Hamill, R. M. Dole and J. Perlwitz, “A multiscale analysis of the extreme weather events over western Russia and northern Pakistan during July 2010,” Monthly Weather Review, vol. 140 no. 5, pp. 1639-1664, 2012, available at https://journals.ametsoc.org/view/journals/mwre/140/5/mwr-d-11-00191.1.xml?tab_body=pdf

34) S. Kreft, D. Eckstein and I. Melchior, “Global climate risk index 2017. Who suffers most from extreme weather events? Weather-related loss events in 2015 and 1996 to 2015,” Germanwatch. Germany, 2016, available at https://policycommons.net/artifacts/1555054/global-climate-risk-index-2017/2244863/fragments/?page=2

35) Pakistan Meteorological Department, (PMD), “ A Report on the implementation of diagnostic study for 2010 flood and extreme moon soon rains 2011 in Pakistan under sustainable development through peace building, governance and economic recovery in KP and support landslide IDPs in Hunza Nagar and Gilgit district when UNDP serves as implementing partner,” 2012, available at http://www.pmd.gov.pk/en/research-development/reports/flood_diagnostic_2010_2011.pdf

36) A. Raza, “Lahore baking in hottest April since 1993,” The News International, 2017, available at https://www.thenews.com.pk/print/199174-Lahore-baking-in-hottest-April-since-1993

37) R. Merz and G. Blöschl, “A process typology of regional floods,” Water resources research, vol. 39, no. 12, 2003, available at https://agupubs.onlinelibrary.wiley.com/doi/full/10.1029/2002WR001952

38) M. Imran and A. Mehmood, “Analysis and mapping of present and future drivers of local urban climate using remote sensing: a case of Lahore, Pakistan,” Arabian Journal of Geosciences, vol. 13, no. 6, pp. 1-14, 2020, available at https://link.springer.com/article/10.1007/s12517-020-5214-2

39) NOAA National Centers for Environmental Information, “State of the Climate: Monthly Global Climate Report for Annual 2015,” 2016, available at https://www.ncei.noaa.gov/access/monitoring/monthly-report/global/201513.

40) A. A. Kafy, M. Islam, S. Sikdar, T. J. Ashrafi, A. Al-Faisal, M. A. Islam, A. Al Rakib, M.H.H. Khan, M. H. S. Sarker. And M. Y. Ali, “Remote sensing-based approach to identify the influence of land use/land cover change on the urban thermal environment: a case study in Chattogram City, Bangladesh,” In *Re-Envisioning Remote Sensing Applications,* pp. 217-240. CRC Press, 2021, available at https://www.taylorfrancis.com/chapters/edit/10.1201/9781003049210-16/remote-sensing-based-approach-identify-influence-land-use-land-cover-change-urban-thermal-environment-abdulla-al-kafy-muhaiminul-islam-soumik-sikdar-tahera-jahan-ashrafi-abdullah-al-faisal-md-arshadul-islam-abdullah-al-rakib-md-hasib-hasan-khan-md-hasnan-sakin-sarker-md-yeamin-ali

41) Y. Feng, H. Li, X. Tong, L. Chen and Y. Liu, ‘Projection of land surface temperature considering the effects of future land change in the Taihu Lake Basin of China,” Global and Planetary Change, vol. 167, pp. 24-34, 2018, available at https://doi.org/10.1016/j.gloplacha.2018.05.007

42) F. O. Akinyemi, M. Ikanyeng, J. Muro, “ Land cover change effects on land surface temperature trends in an African urbanizing dryland region,” City and environment interactions, vol. 4, p. 100029, 2019, available at https://doi.org/10.1016/j.cacint.2020.100029

43) F. Liu, X. Jia., W. Li, A. Du and D. Wang, “Analysis of land surface temperature evolution based on regional road scope,” Advances in Civil Engineering, vol. 20, 2020, available at https://www.hindawi.com/journals/ace/2020/4350787/

44) C. Y. Wai, N. Muttil, M. A. U. R. Tariq, P. Paresi, R. C. Nnachi and A. W. Ng, “Investigating the Relationship between Human Activity and the Urban Heat Island Effect in Melbourne and Four Other

International Cities Impacted by COVID-19," Sustainability, vol. 14 no. 1, p. 378, 2021, available at https://www.mdpi.com/2071-1050/14/1/378/htm

45) G. Roshan, R. Sarli, and S. W. Grab, "The case of Tehran's urban heat island, Iran: Impacts of urban 'lockdown' associated with the COVID-19 pandemic," Sustainable Cities and Society, vol. 75, p. 103263, 2021, available at https://doi.org/10.1016/j.scs.2021.103263

46) A. S. Alqasemi, M. E. Hereher, G. Kaplan, A. M. F. Al-Quraishi, H. Saibi, "Impact of COVID-19 lockdown upon the air quality and surface urban heat island intensity over the United Arab Emirates," Science of The Total Environment, vol. 767, p. 144330, 2021, available at https://www.sciencedirect.com/science/article/pii/S004896972037861X

47) Z. Liu, J. Lai, W. Zhan, B. Bechtel, J. Voogt, J. Quan, L. Hu, P. Fu, F. Huang, L. Li, and Z. Guo, "Urban heat islands significantly reduced by COVID-19 lockdown," Geophysical Research Letters, vol. 49, no. 2, p.e2021GL096842, 2022, available at https://doi.org/10.1029/2021GL096842

48) F. Mumtaz, Y. Tao, G. de Leeuw, L. Zhao, C. Fan, A. Elnashar, B. Bashir, G. Wang, L. Li, S. Naeem and A. Arshad, "Modeling spatio-temporal land transformation and its associated impacts on land surface temperature (LST)," Remote Sensing, vol. 12, no. 18, p.2987, 2020, available at https://www.mdpi.com/2072-4292/12/18/2987

49) S. Fahad, W. Li, A.H. Lashari, A. Islam, L.H. Khattak and U. Rasool, "Evaluation of land use and land cover Spatio-temporal change during rapid Urban sprawl from Lahore, Pakistan," Urban Climate, vol. 39, p. 100931, 2021, available at https://www.sciencedirect.com/science/article/abs/pii/S2212095521001619

50) J. Ngarambe, S. J., Joen, C. H. Han and G. Y. Yun, "Exploring the relationship between particulate matter, CO, SO2, NO2, O3 and urban heat island in Seoul, Korea," Journal of Hazardous Materials, vol. 403, p. 123615, 2021, available at https://www.sciencedirect.com/science/article/abs/pii/S0304389420316010?via%3Dihub

51) S. Peng, Z. Feng, H. Liao, B. Huang, S. Peng, and T. Zhou, "Spatial-temporal pattern of, and driving forces for, urban heat island in China," Ecological indicators, vol. 96, pp. 127-132, 2019, available at https://doi.org/10.1016/j.ecolind.2018.08.059

52) M. Santamouris, "Analyzing the heat island magnitude and characteristics in one hundred Asian and Australian cities and regions, "Science of the Total Environment, vol. 512, pp. 582-598, 2015, available at https://www.sciencedirect.com/science/article/abs/pii/S0048969715000753?via%3Dihub

53) E. A. Ramírez-Aguilar and L. C. L. Souza, "Urban form and population density: Influences on Urban Heat Island intensities in Bogotá, Colombia," Urban Climate, vol. 29, pp. 100497, 2019, available at https://www.sciencedirect.com/science/article/abs/pii/S2212095519300653?via%3Dihub